Influence of sea ice decline, atmospheric warming, and glacier width on marine-terminating outlet glacier behavior in northwest Greenland at seasonal to interannual timescales

Carr, J Rachel ; Vieli, Andreas ; Stokes, Chris R

Abstract: Discharge from marine-terminating outlet glaciers represents a key component of the Greenland Ice Sheet mass budget and observations suggest that mass loss from northwest Greenland has recently accelerated. Despite this, the factors controlling outlet glacier dynamics within this region have been comparatively poorly studied. Here we use remotely sensed data to investigate the influence of atmospheric, oceanic, and glacier-specific controls on the frontal position of Alison Glacier (AG), northwest Greenland, and nine surrounding outlet glaciers. AG retreated by 9.7 km between 2001 and 2005, following at least 25 years of minimal change. Results suggest that sea ice and air temperatures influence glacier frontal position at seasonal and interannual timescales. However, the response of individual outlet glaciers to forcing was strongly modified by factors specific to each glacier, specifically variations in fjord width and terminus type. Overall, our results underscore the need to consider these factors in order to interpret recent rapid changes and predict the dynamic response of marine-terminating outlet glaciers to atmospheric and oceanic forcing.

DOI: https://doi.org/10.1002/jgrf.20088

JOURNAL OF GEOPHYSICAL RESEARCH: EARTH SURFACE, VOL. 118, 1–17, doi:10.1002/jgrf.20088, 2013

Influence of sea ice decline, atmospheric warming, and glacier width on marine-terminating outlet glacier behavior in northwest Greenland at seasonal to interannual timescales

J. Rachel Carr,[1] Andreas Vieli,[1] and Chris Stokes[1]

Received 6 November 2012; revised 23 April 2013; accepted 2 June 2013.

[1] Discharge from marine-terminating outlet glaciers represents a key component of the Greenland Ice Sheet mass budget and observations suggest that mass loss from northwest Greenland has recently accelerated. Despite this, the factors controlling outlet glacier dynamics within this region have been comparatively poorly studied. Here we use remotely sensed data to investigate the influence of atmospheric, oceanic, and glacier-specific controls on the frontal position of Alison Glacier (AG), northwest Greenland, and nine surrounding outlet glaciers. AG retreated by 9.7 km between 2001 and 2005, following at least 25 years of minimal change. Results suggest that sea ice and air temperatures influence glacier frontal position at seasonal and interannual timescales. However, the response of individual outlet glaciers to forcing was strongly modified by factors specific to each glacier, specifically variations in fjord width and terminus type. Overall, our results underscore the need to consider these factors in order to interpret recent rapid changes and predict the dynamic response of marine-terminating outlet glaciers to atmospheric and oceanic forcing.

Citation: Carr, J. R., A. Vieli, and C. Stokes (2013), Influence of sea ice decline, atmospheric warming, and glacier width on marine-terminating outlet glacier behavior in northwest Greenland at seasonal to interannual timescales, *J. Geophys. Res. Earth Surf.*, *118*, doi:10.1002/jgrf.20088.

1. Introduction

[2] Numerous studies have documented rapid mass loss from the Greenland Ice Sheet (GrIS) during the past 20 years [e.g., *Jacob et al.*, 2012; *Rignot and Kanagaratnam*, 2006; *Sasgen et al.*, 2012; *van den Broeke et al.*, 2009], with deficits accelerating by $20.1 \pm 1\,\mathrm{km}^3\ \mathrm{a}^{-2}$ between 1992 and 2010 [*Rignot et al.*, 2011]. This loss was attributed approximately equally to negative surface mass balance, primarily resulting from an increase in surface melting relative to accumulation, and increased ice discharge from marine-terminating outlet glaciers [*Rignot et al.*, 2008; *Rignot et al.*, 2011; *van den Broeke et al.*, 2009]. Indeed, observations have demonstrated that outlet glaciers can undergo rapid dynamic change and produce substantial mass loss at annual to decadal timescales [*Bevan et al.*, 2012; *Howat et al.*, 2008; *Joughin et al.*, 2012; *Pritchard et al.*, 2009; *Rignot et al.*, 2008]. Consequently, understanding the factors controlling Greenland outlet glacier dynamics is crucial for accurate prediction of near-future sea-level rise and GrIS response to climate change [*Intergovernmental Panel on Climate Change*, 2007].

[3] At present, considerable uncertainty remains over the primary drivers of Greenland outlet glacier behavior, with potential controls including air temperatures, ocean temperatures, sea ice, and factors specific to individual glaciers, such as basal topography, fjord geometry, glacier velocity, width, and catchment area [*Carr et al.*, 2013]. Here we use the term "oceanic" to refer to forcing associated with sea ice, sea surface temperatures (SSTs), and subsurface ocean temperatures. Increasing concern over climate warming from the 1990s together with the synchronous nature of Greenland outlet glacier retreat in the early 2000s, particularly in south-eastern Greenland [e.g., *Howat et al.*, 2008; *Murray et al.*, 2010], led researchers to focus on the role of atmospheric and oceanic forcing in driving outlet glacier dynamics. However, recent studies have demonstrated that the response of individual glaciers to these factors can vary substantially at regional scales [*McFadden et al.*, 2011] and that glacier-specific factors, particularly bed topography, may significantly influence Greenland outlet glacier behavior [*Howat et al.*, 2011; *Joughin et al.*, 2010a; *Nick et al.*, 2009; *Thomas et al.*, 2009]. Here we focus specifically on the role of fjord width, terminus type, and, to a lesser extent, basal topography in modulating the response of outlet glaciers to external forcing. Although the potential influence of basal topography on glacier dynamics has been recognized for some time [*Alley*, 1991; *Meier and Post*, 1987; *Weertman*, 1974], it has yet to be widely investigated on the GrIS, due to limited data availability, and other glacier-specific controls, such as fjord width variations, remain poorly studied [*Carr et al.*, 2013]. Understanding the role of these controls is crucial for accurate sea level rise

Additional supporting information may be found in the online version of this article.

[1]Department of Geography, Durham University, Durham, UK.

Corresponding author: J. R. Carr, Department of Geography, Durham University, Science Site, South Road, Durham DH1 3LE, UK. (j.r.carr@durham.ac.uk)

2169-9003/13/10.1002/jgrf.20088

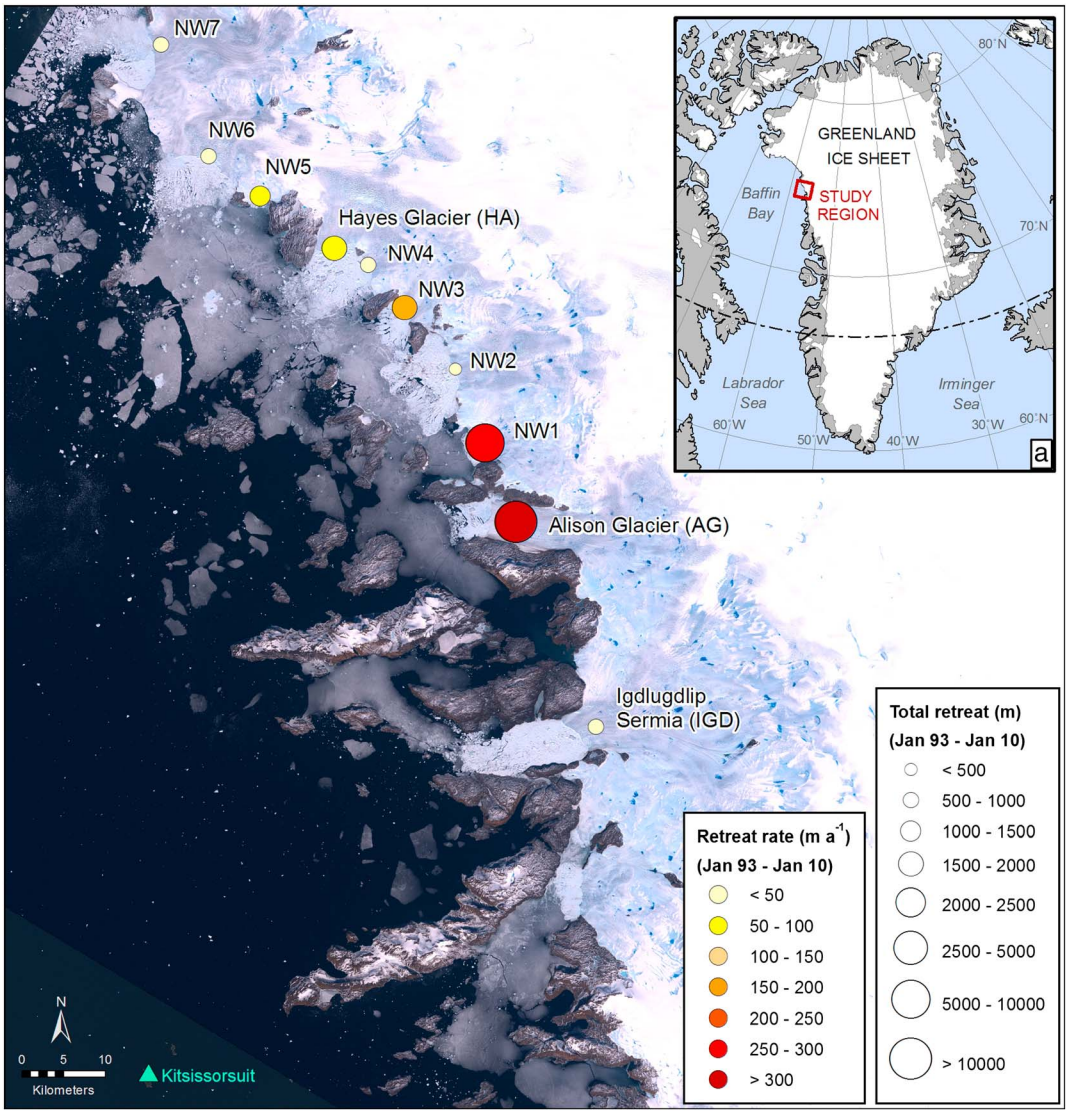

Figure 1. Location of study glaciers, Kitsissorsuit meteorological station (green triangle), and average outlet glacier retreat rate (symbol color) and total retreat (symbol size) between 2 January 1993 and 26 January 2010. Base image: Landsat scene acquired 27 June 2001 and provided by Global Land Cover Facility.

prediction, as mass loss rates are frequently extrapolated from a small number of study glaciers and so inadequate consideration of glacier-specific factors could lead to substantial over- or under-estimates.

[4] Here we investigate the influence of atmospheric, oceanic, and glacier-specific controls on the frontal position of Alison Glacier (AG), northwest Greenland, and its nine neighboring marine-terminating outlet glaciers (Figure 1). Northwest Greenland has undergone rapid mass loss [*Khan et al.*, 2010] and significant changes in glacier dynamics in the past decade [*Kjær et al.*, 2012], including widespread retreat [*Howat and Eddy*, 2011], substantial acceleration [*Moon et al.*, 2012] and an increased frequency of glacial earthquakes [*Veitch and Nettles*, 2012]. We focus particularly on AG as it has recently exhibited exceptionally high retreat rates [*Joughin et al.*, 2010a; *McFadden et al.*, 2011] in comparison to both regional and ice-sheet wide values, yet it has been relatively poorly studied. We first investigate the influence of atmospheric and oceanic forcing on seasonal changes in frontal position between 2004 and 2010. We then assess the relative importance of these controls at interannual timescales for the period 1993 to 2010 and evaluate longer-term glacier behavior from 1976 to present. Finally, we investigate the role of fjord width, terminus type, and basal topography in modulating glacier response to atmospheric and oceanic forcing.

2. Methods

2.1. Glacier Frontal Position

[5] Outlet glacier frontal positions were obtained from a combination of radar and visible satellite imagery from 1976 to 2012. The primary source was Synthetic Aperture Radar (SAR) Image Mode Precision imagery, acquired as part of the ERS1, ERS2, and Envisat missions and provided by the European Space Agency (ESA). Scenes were selected

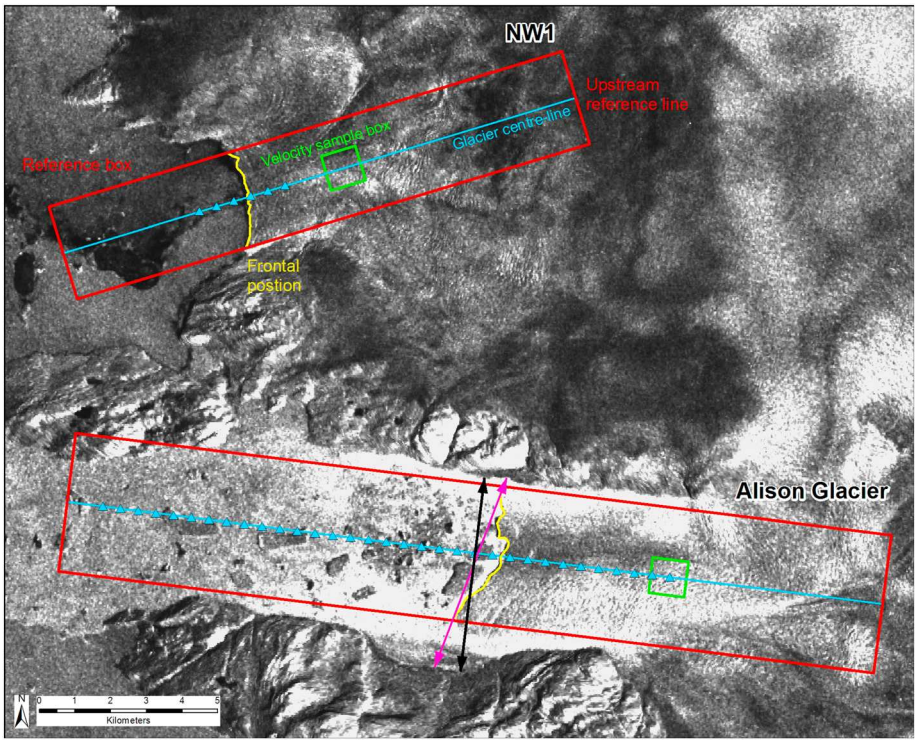

Figure 2. Illustration of the method used for measuring outlet glacier frontal positions, ice velocities, and fjord width. A reference box was defined which extends parallel to the main ice flow direction from an arbitrary upstream reference line (red box), and the glacier terminus was repeatedly digitized from successive images (yellow line). Mean ice velocities were sampled within a 1 km^2 box (green box), orientated parallel to and centered on the glacier centerline (blue line). Blue dots indicate sampling locations for fjord width perpendicular to the centerline. Fjord width was measured (i) perpendicular to the glacier centerline (black line) at 500 m intervals from the upstream reference line (blue triangles) and (ii) approximately parallel to the glacier terminus for each available terminus position (pink line). The base image provides a typical example of an ENVISAT scene used for terminus mapping and shows the ice mélange and calving of large, tabular icebergs from the terminus of Alison Glacier during its rapid retreat phase. Base image: ENVISAT ASAR image, acquired 2 October 2004, courtesy of ESA (European Space Agency).

as close to the end of the calendar month as possible to allow for comparison with monthly climatic and oceanic data. The images were processed by applying precise orbital state vectors, provided by the ESA, and radiometric calibration was applied. Images were then multilooked to reduce speckle and were terrain corrected using Version 2 of the 30 m resolution Advanced Spaceborne Thermal Emission and Reflection Radiometer Global Digital Elevation Model. ERS images were coregistered with corresponding Envisat scenes, which have a higher geolocation accuracy. Processed scenes were output at a spatial resolution of 37.5 m. Where possible, periods of limited SAR Image Mode data availability were supplemented with Landsat data obtained from the Global Land Cover Facility (http://glcf.umiacs.umd.edu/), the USGS Global Visualization Viewer (http://glovis.usgs.gov/) and USGS Earth Explorer (http://earthexplorer.usgs.gov/). Frontal positions from 1976 were obtained from Landsat MSS images acquired on 22 March (IGD) and 9 April (other glaciers) 1976. Frontal positions for 1986 were identified from a SPOT-1 panchromatic image, acquired on 9 August 1986).

[6] Adopting previous methods [*Howat et al.*, 2010; *Howat et al.*, 2008; *McFadden et al.*, 2011; *Moon and Joughin*, 2008], changes in terminus position were calculated by repeatedly digitizing the ice front within a reference box of fixed width (Figure 2). The edges of the reference box were orientated approximately parallel to the main ice flow direction and were joined by a reference line at an arbitrary distance up-glacier (Figure 2). The glacier terminus was digitized from sequential images, and the mean change in frontal position was calculated by dividing the change in the area of the reference box by its width. This method improves upon using a single centerline reference point, as it accounts for uneven changes in the ice front and provides a more representative measure of frontal position change [*Howat et al.*, 2008; *Moon and Joughin*, 2008]. Total retreat and retreat rates were calculated relative to 2 January 1993, which was the earliest image available for all of the study glaciers. Due to data availability, the temporal resolution of the frontal positions varied during the study period: data were available at a decadal resolution between 1976 and 1992, at subannual to annual resolution between 1993 and 2003 and at approximately monthly intervals between 2004 and 2010.

[7] Potential sources of error in frontal position are: (i) coregistration of ERS and Envisat images; (ii) geolocation accuracy of Envisat data; (iii) relative geolocation accuracy of ERS/Envisat and visible imagery; and (iv) manual digitizing errors. The error associated with coregistration was assessed

by manually checking the coregistration of each ERS scene against its partner Envisat image: ERS scenes that did not coregister at the imagery resolution were rejected. On the basis of previous geolocation accuracy assessments, errors in Envisat geolocation are likely to be substantially less than the image resolution [*Small et al.*, 2004]. The relative geolocation of the radar and visible imagery, and manual digitizing errors, were evaluated by repeatedly digitizing 22 sections of rock coastline from a subsample of five ERS, five Envisat, and five Landsat images, where there should be no discernible change in coastline position between scenes. The resultant total mean error in frontal position was 28.9 m, which is below the image resolution and can be primarily attributed to manual digitizing. Due to their comparatively poor original georeferencing, the two Landsat MSS images were georeferenced to a later Landsat image (acquired on 27 June 2001) using distinctive features on the rock coastline. The resultant root mean square error was 62 m for the image acquired on the 22 March 1976 and 78 m for the image from 9 April 1976.

2.2. Glacier and Fjord Width

[8] The initial terminus width of each study glacier was measured from the earliest common image from 2 January 1993. Terminus width was measured by drawing a line approximately parallel to each calving front and measuring the distance between the two points where the line intersected with the lateral margins of the terminus at sea level. Fjord width was measured in two ways. First, lines were drawn perpendicular to the glacier centerline at intervals of 500 m from the upstream reference line, and fjord width was measured between the two points where the lines intersected with the fjord walls at sea level (Figure 2). Second, lines were drawn approximately parallel to the calving front using each available frontal position and fjord width was measured between the points where the lines intersected with the fjord walls at sea level (Figure 2). NW1 retreated inland of its fjord during the study period and fjord width was therefore only measured in the section where the terminus was between the fjord walls. Furthermore, width was not measured perpendicular to the calving front, as it became highly concave toward the end of the study period which precluded accurate width measurements using this approach.

2.3. Outlet Glacier Velocities

[9] Ice velocity data were extracted at two time steps (winter 2000–2001 and winter 2005–2006) from the annual ice-sheet-wide velocity maps for the GrIS, developed as part of the NASA Making Earth Science Data Records for Use in Research Environments (MEaSUREs) program [*Joughin et al.*, 2010b]. The velocity data were derived using Interferometric SAR data from the RADARSAT-1 satellite. Mean ice velocities were sampled within a 1 km^2 box, which was centered on and orientated parallel to the glacier centerlines and located 1 km from the glacier terminus, as identified from the winter 2005–2006 velocity map (Figure 2).

2.4. Subglacial Topography

[10] Subglacial topographic data were supplied by Center for Remote Sensing of Ice Sheets (CReSIS) (ftp://data.cresis.ku.edu/data). The Level 2 "Ice Thickness," "Ice Surface," and "Ice Bottom" elevations products were used, which provides measurements of ice-bottom elevations along a series of flightlines across the GIS. Here we used the 2010 Greenland P-3 data set, which was collected between 19 and 21 May 2010 as part of Operation IceBridge aircraft surveys, using the Multichannel Coherent Radar Depth Sounder sensor on the NASA P-3B platform. This data set was selected as it provided the best spatial coverage and data quality within the study region. Data were available for one flightline perpendicular to the coastline and six parallel to the coastline, which were spaced between 2 and 5 km apart. The along-track sample spacing was approximately 14.5 m, and the along-track horizontal resolution was approximately 25 m (http://nsidc.org/data/docs/daac/icebridge/irmcr2/index.html). The depth resolution of the data was 4.5 m. In-built quality flags identify data points as a high, medium, and low confidence pick: this information was used to exclude all data points that were medium or low confidence. Landsat imagery was then used to remove any data points acquired over ocean or land. Further information on data processing, error sources, and specific errors associated with the 2010 Greenland P-3 data are available from http://nsidc.org/data/docs/daac/icebridge/irmcr2/index.html.

2.5. Atmospheric and Oceanic Data

[11] Atmospheric and oceanic data were compiled from a variety of sources and seasonal and monthly means were calculated for comparison with glacier frontal position data. Surface air temperature (SAT) data were obtained from Kitsissorsuit meteorological station (57°49′36″W 74°1′58″N; Figure 1) and were provided by the Danish Meteorological Institute (DMI) at a three-hourly temporal resolution [*Carstensen and Jørgensen*, 2011]. Data were filtered to account for missing values and were only used in the calculation of monthly/annual averages if the following criteria were met [*Cappelen*, 2011]: (i) no more than two consecutive records were missing in a day; (ii) no more than three records in total were missing in a day; (iii) daily averages were available for 22 or more days per month; and (iv) monthly averages were available for all months of the year. The filtered data were then used to calculate mean monthly, summer (JJA), and annual air temperatures and the number of positive degree days (PDDs) per year.

[12] In order to assess the extent to which temperature data at Kitsissosuit are representative across the study region, a latitudinal lapse rate was calculated using mean monthly data from DMI meteorological stations at Nuusuaq (located 386 km south of Kitsissosuit) and Kitsussut (located 512 km north of Kitsissosuit). The estimated lapse rate was 0.004°C/km, which equates to a mean temperature difference of 0.43°C between Kitsissosuit and the most northerly glacier, NW7. This value is substantially smaller than the magnitude of interannual warming, and we focus primarily on air temperature trends, rather than absolute values. At seasonal timescales, we focus on IGD, AG, and NW1, which are the closest to Kitsissosuit, and the mean air temperature difference between these glaciers was minimal (0.14°C). Furthermore, our frontal position data are at a monthly temporal resolution, so potential differences in seasonal retreat due to a later onset of melt towards the north of the transect are unlikely to be detectable within the data resolution.

[13] Sea ice data were extracted from charts provided by the National Ice Center, which were compiled from a range of directly measured and remotely sensed data sources (http://www.natice.noaa.gov/). Various imagery sources are incorporated into the charts, including Envisat, Defense Meteorological Satellite Program Operational Linescan System, Advanced Very High Resolution Radiometer, and RADARSAT, which have a spatial resolution down to 50 m. Data are provided at a weekly to biweekly temporal resolution, and the accuracy of sea ice concentrations is estimated to be ± 10% [*Partington et al*., 2003]. The data set uses information from multiple sensors and manual interpretation, which generally provides more accurate sea ice information than a single data source.

[14] Data were sampled at each study glacier from a polygon extending the full width of the terminus and 50 m perpendicular to it, in order to extract sea ice concentrations from as close to the terminus as possible. For the seasonal analysis, monthly means were calculated for each study glacier. Sea ice data from all study glaciers were then used to calculate monthly and seasonal means for the study region. On average, monthly and seasonal means for individual glaciers varied from the regional average by 3.2% and 3.8%, respectively, suggesting that sea ice concentrations do not vary substantially across the region and that regional means are representative of conditions at each study glacier. Regional averages were also used to calculate the number of ice-free months per year, which are defined as months when mean monthly sea ice concentrations are equal to zero.

[15] Monthly SST data were obtained from the Moderate Resolution Imaging Spectrometer (MODIS), provided by the NASA Ocean Color Project (http://oceancolor.gsfc.nasa.gov/), and from Version 2 of the Reynolds SST analysis data set [*Reynolds et al*., 2007]. SST data were used to investigate surface ocean temperatures only and are not necessarily representative of conditions at depth. MODIS data were used for the period 2000 to 2010 and have a spatial resolution of 5 km. The in-built data quality mask was used to remove pixels flagged as low quality and a combination of Landsat imagery, and the in-built land mask were used to remove land pixels. SSTs were then sampled from all grid squares located within 25 km of each study glacier terminus.

[16] As MODIS data were only available from 2000 onwards, Reynolds SST analysis data were also used to assess interannual changes in SSTs. However, the Reynolds data have a comparatively coarse spatial resolution (0.25°) and MODIS data were therefore used for the more detailed seasonal analysis between 2004 and 2010. The in-built mask was used to remove pixels identified as land and sea ice and values were sampled from the grid squares closest to the glacier termini. Both data sets were sampled as close to the termini as possible, as SSTs proximal to the glaciers are likely to be strongly affected by local factors such as sea ice, glacial meltwater discharge and icebergs. Monthly values from each data set were then used to calculate mean July–September SSTs for the study region, as these months were identified as ice free in the data quality masks for both data sets for all years.

[17] In addition to the SST data, subsurface ocean temperatures were obtained from the Hadley Centre EN3 quality controlled subsurface ocean temperature and salinity data set [*Ingleby and Huddleston*, 2007], which is available at a monthly temporal resolution. Data were sampled from the 1° by 1° model grid square that was located closest to the study glaciers, situated at a distance of 37 to 71 km from the glacier termini. The data provide information on ocean temperatures on the continental shelf and do not account for the complex processes within the glacier fjords or at the calving front. The data are therefore unsuitable for assessing oceanic conditions at the glacier front and instead are used to give a general indication of temperature change with depth in the water column at the continental shelf.

3. Results

3.1. Outlet Glacier Frontal Position

3.1.1. Seasonal Variation

[18] The temporal resolution of the data allows for analysis of seasonal frontal position variations from 2004 onwards. Data are presented for AG, NW1, and IGD (Figure 3), which encompass the range of the different types of seasonal frontal position variation and response to forcing within the study region (seasonal data for the other study glaciers are provided in the auxiliary material). The onset of seasonal retreat within the study region usually begins between April and July and seasonal advance generally commences between the end of August and the end of November (Figure 3). However, there is substantial variation in the timing of seasonal advance/retreat, both on individual glaciers and across the study region (Figure 3). With the exception of AG and NW1, seasonal frontal position variation within the study area averaged approximately ±400 m and ranged between ±660 m at Hayes Glacier and ±210 m at NW6. Aside from AG and NW1, the magnitude of seasonal retreat varied little from year-to-year and seasonal variations were significantly greater than the interannual trend, despite an overall pattern of retreat (Figures 1 and 3). In contrast, the amount of seasonal retreat at AG fluctuated substantially over the study period: during the summers of 2004 and 2005, the glacier retreated by 3.61 km and 2.29 km, respectively, and underwent little seasonal advance (Figure 3a). In contrast, seasonal retreat in 2008 and 2009 amounted to only 0.89 km and 0.50 km, respectively (Figure 3a). The magnitude of seasonal retreat at NW1 also showed substantial interannual variation and reached a maximum of 1.7 km in summer 2005. Subsequent to winter 2004, seasonal retreat at NW1 was generally far greater than seasonal advance (Figure 3d). To obtain an approximate estimate of winter calving, we compared seasonal advance rates and ice velocities in winter 2005–2006. AG, NW1, and a number of the other study glaciers advanced at a rate which was very similar to their flow speed (Table 1), suggesting that winter calving was minimal. However, the rate of winter advance was considerably less than the terminus velocity on other glaciers, including IGD, NW2, and NW7 (Table 1), indicating that calving may have persisted during the winter.

3.1.2. Interannual Variation

[19] Due to data availability, interannual glacier retreat was compared to atmospheric and oceanic forcing data between 1993 and 2010, and the limited number of frontal positions available prior to 1992 were used to provide a longer-term context. Between 1993 and 2010, all study

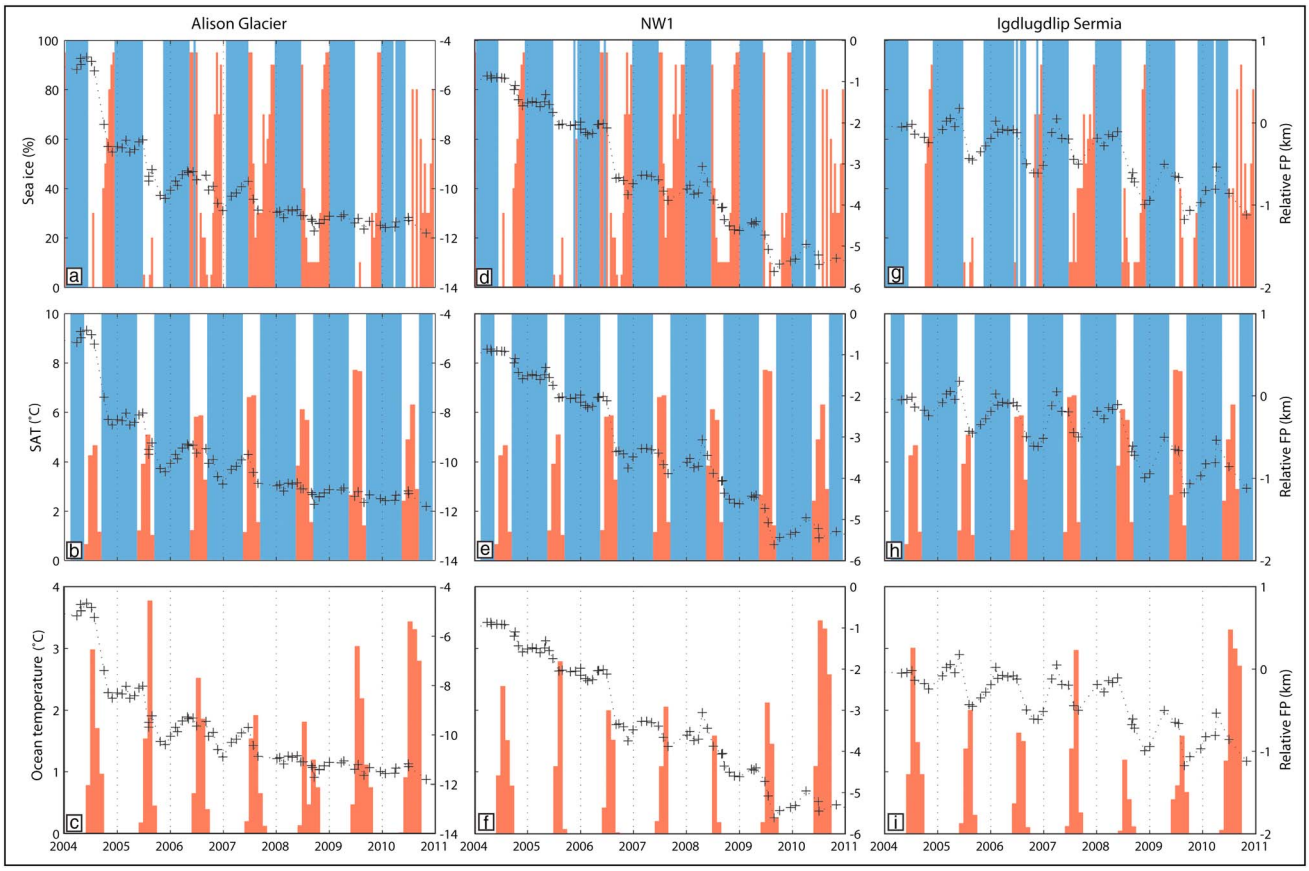

Figure 3. Outlet glacier frontal position (black crosses) and seasonal atmospheric and oceanic forcing factors at (left) Alison Glacier, (middle) NW1, and (right) IGD. (a, d, and g) Mean monthly sea ice concentrations plotted in percent, with fast ice (i.e., 100%) in blue and all other values in red. (b, e, and h) Mean monthly air temperatures for Kitsissorsuit meteorological station, plotted in red for temperatures above 0°C and blue for temperatures below 0°C. (c, f, and i) Mean monthly sea surface temperatures (SST) from MODIS data.

glaciers underwent net retreat, which predominantly occurred during the past decade, and the magnitude of retreat varied dramatically between glaciers (Table 1 and Figures 1 and 4a). At AG, both the rate and magnitude of retreat far exceeded the regional average, with retreat totaling 11.6 km between 1993 and 2010. Approximately 10 km (84%) of the total retreat at AG occurred between July 2001 and October 2005, and retreat rates peaked

Table 1. Summary of Glacier Retreat Rates for January 1993 to January 2010, April 1976 to June 2001, and June 2001 to January 2010[a]

Glacier	Total Retreat (m)	Retreat Rate (m a^{-1})	Retreat Rate (m a^{-1})	Retreat Rate (m a^{-1})	Glacier Velocity	Glacier Velocity	Velocity Change	Ice Front Advance Rate
	(1993–2010)	(1993–2010)	(1976–2001)	(2001–2010)	(winter 2000–2001)	(winter 2005–2006)	(winter January 2000 to June 2005)	(winter June 2005)
NW7	749	42	-	-	1090	950	−140	212
NW6	665	37	6	63	800	670	−130	422
NW5	1152	64	30	60	90	100	+10	-
HA	1768	98	7	106	2160	2070	−90	1353
NW4	668	37	7	53	850	830	−20	814
NW3	1925	107	10	179	1060	1050	−10	1025
NW2	196	11	121	15	2710	2480	−230	675
NW1	5317	295	263	551	390	450	+60	653
AG	11,575	643	0	1227	1800	2840	+1040	2687
IGD	824	46	+3	108	2680	2760	+80	1136

[a]Glaciers are ordered by location, from north to south (see Figure 1), and abbreviations are as follows: AG (Alison Glacier); HA (Hayes Glacier); and Igdlugdlip Sermia (IGD). The total mean error in frontal position is 28.9 m, equating to a mean error in retreat rate of 1.6 m a^{-1}. Ice velocities are shown for winter 2000–2001 and 2005–2006 and are used to calculate change in glacier velocity between the two time periods. Velocities were obtained the MEaSUREs ice-sheet-wide velocity maps [*Joughin et al.*, 2010b]. Winter ice front advance rates are shown for 2005–2006 and were calculated from glacier frontal position data. Note the markedly higher retreat rates on AG and NW1 in comparison to the other study glaciers.

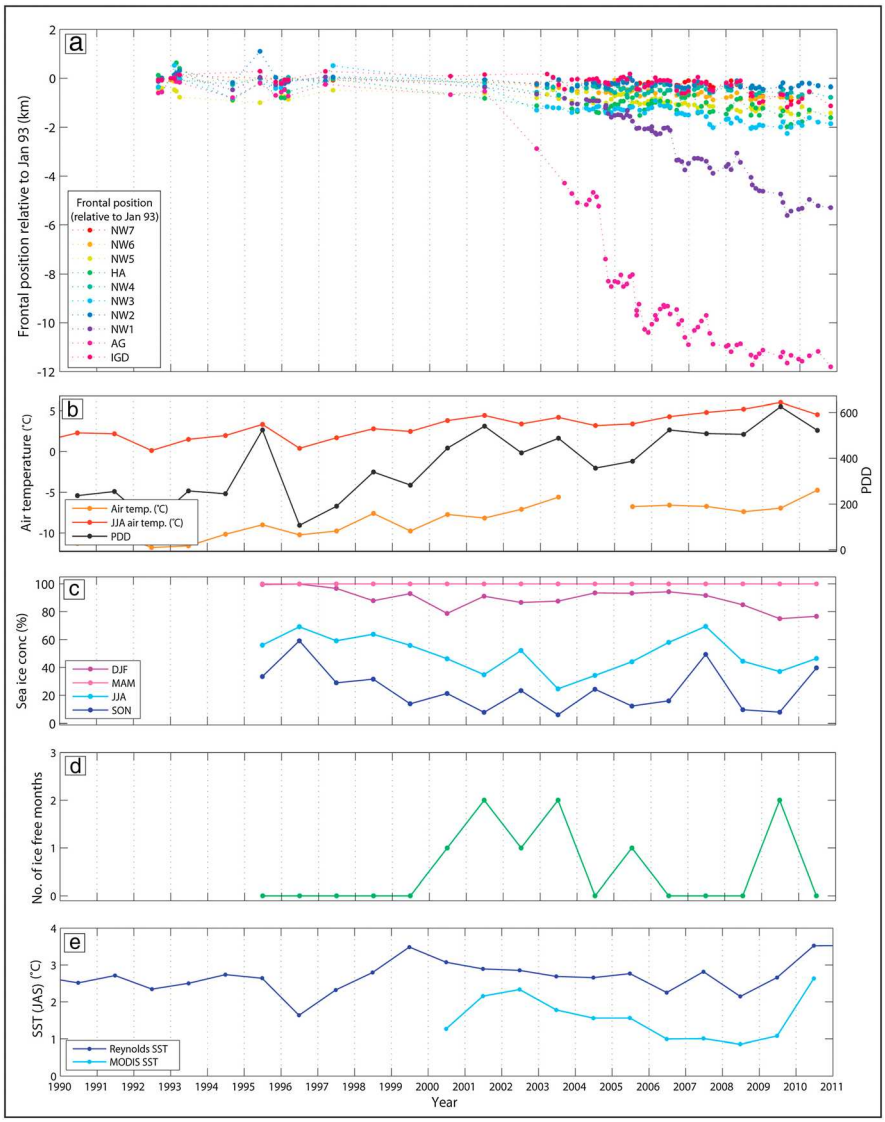

Figure 4. Relative glacier frontal position and climatic/oceanic forcing factors. (a) Frontal position for all glaciers, relative to January 1993, color coded according to glacier. (b) Mean annual and mean summer (JJA) air temperatures and number of positive degree days (PDD) at Kitsissorsuit meteorological station. (c) Mean seasonal sea ice concentrations for all study glaciers for the periods December–February (DJF), March–May (MAM), June–August (JJA), and September–November (SON). (d) Number of months of ice-free conditions for all study glaciers. (e) Mean sea surface temperatures for July–September (JAS) from MODIS (light blue) and Reynolds (dark blue) SST data.

between July and October 2004, when the glacier retreated over 3 km (Figures 1 and 4a). Retreat was accompanied by a 63% increase in ice velocities at AG's terminus between winter 2000–2001 and 2005–2006 (Table 1). At NW1, frontal position varied little between 1992 and 2001, and retreat rates were low (24.8 m a^{-1}) (Figure 4a). Retreat rates then increased in two phases: retreat averaged 221.2 m a^{-1} between June 2001 and July 2006 and increased to 352.5 m a^{-1} thereafter (Figure 4a). The most rapid retreat at NW1 occurred between July 2006 and September 2006, when the glacier retreated by 1.2 km, and rapid retreat phases also occurred during the summers of 2008 and 2009.

[20] The other study glaciers began to retreat from 2001 onwards (Figures 1 and 4a), but the magnitude of total retreat was smaller (200 m to 2 km) and average retreat rates were slower (10 to 100 m a^{-1}) than at AG or NW1 (Table 1 and Figures 1 and 4a). Although the overall trend was one of retreat, it was comparatively gradual on these glaciers, and interannual retreat rates were significantly less than the seasonal variability in frontal position. Between January 2000 and June 2005, the glaciers underwent minimal acceleration near to the terminus, and a number of glaciers underwent slight deceleration (Table 1). Two patterns of interannual retreat are therefore apparent within the study region between 1993 and 2010: (i) rapid, nonlinear, step-wise recession, which results in high-magnitude retreat at interannual timescales and occurred at AG and NW1; and (ii) slower, more gradual retreat, which produces far lower total retreat rates and occurred on the remaining study glaciers.

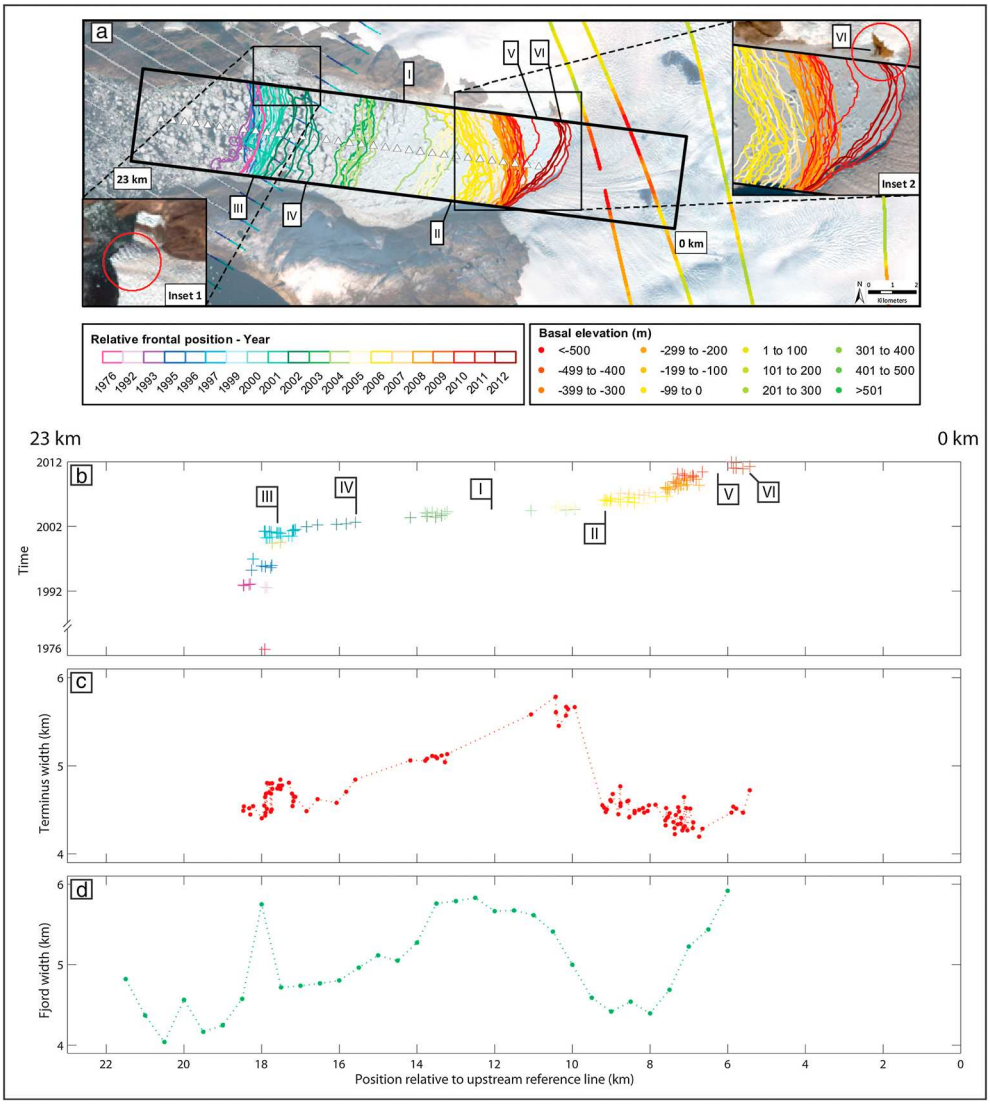

Figure 5. Frontal position of Alison Glacier in relation to basal elevation, fjord width parallel to the glacier terminus, and fjord width perpendicular to the centerline. (a): AG frontal position over time (colored lines) in relation to ice-bottom elevations from CReSIS radar depth sounder flightlines, color coded from green (high elevation) to red (low elevation). Labeled positions are discussed in the text. Base image: Landsat scene acquired 11 September 2011 and provided by USGS GLOVIS. (b) AG frontal position over time (colored crosses), relative to upstream reference line. (c) Fjord width parallel to the glacier terminus for each available frontal position. (d) Fjord width perpendicular to the centerline at 500 m intervals from the upstream reference line (sample locations indicated by white triangles in Figure 5a).

[21] Frontal positions on the majority of the study glaciers showed little net change between 1976 and 2001 (Figures 5 and 6), and their retreat rates were substantially lower than between 2001 and 2010 (Table 1). Exceptions to this were NW1 and NW2 (Figure 2 and Table 1), which retreated by approximately 6 km and 3 km, respectively, between 1976 and 2001, with the majority of retreat occurring prior to 1986. The western margin of NW7 also retreated during this period, coincident with the loss of a section of ice located to the west of the lateral margin of the glacier. At AG, the terminus position changed very little between 1976 and 2001 (Figure 5 and Table 1): results show a net advance of 9 m during this interval, which equates to a rate of 0.4 m a^{-1}, and is significantly less than the frontal position error. Three distinct phases of frontal position behavior are therefore apparent at AG: (i) minimal net retreat between June 1976 and July 2001; (ii) very rapid retreat between July 2001 and October 2005 at 2431.4 m a^{-1}; and (iii) more gradual retreat at 306.2 m a^{-1} until the end of the study period (Figure 5). The vast majority of retreat on AG and on the other study glaciers occurred from 2001 onwards.

3.2. Atmospheric and Oceanic Forcing

[22] Mean annual surface air temperature at Kitsissorsuit increased by almost 8°C between 1990 and 2010 (Figure 4b), which equates to a linear warming trend of 0.29°C per year ($R^2 = 0.79$). This trend concurs with substantial increases in air temperature observed at nearby meteorological stations

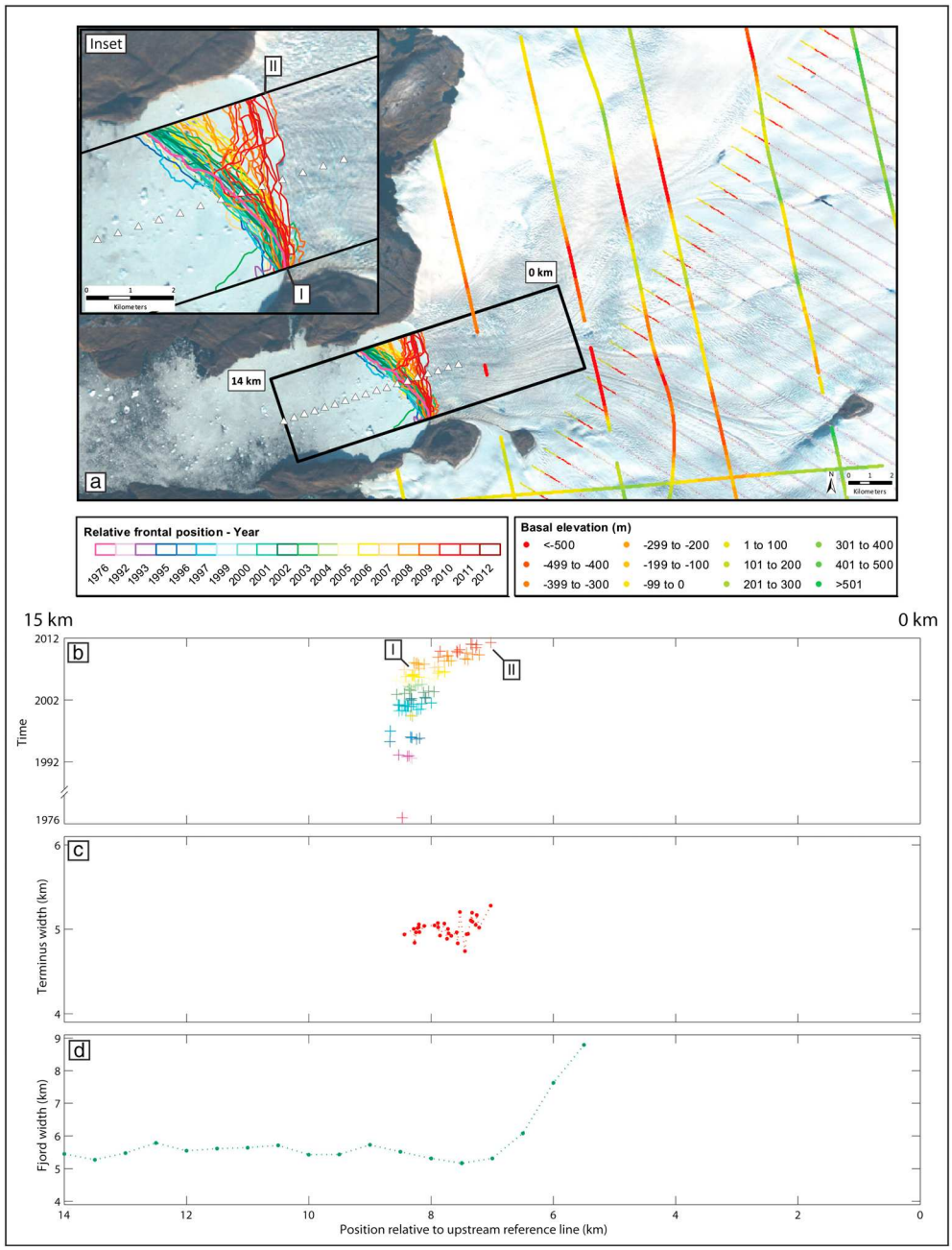

Figure 6. Frontal position of Igdlugdlip Sermia in relation to basal elevation, fjord width parallel to the glacier terminus, and fjord width perpendicular to the centerline. (a) IGD frontal position over time (colored lines) in to ice-bottom elevations from CReSIS radar depth sounder flightlines, color coded from green (high elevation) to red (low elevation). Labeled positions are discussed in the text. Base image: Landsat scene acquired 11 September 2011 and provided by USGS GLOVIS. (b) IGD frontal position over time (colored crosses), relative to upstream reference line. (c) Fjord width parallel to the glacier terminus, for each available frontal position. (d) Fjord width perpendicular to the centerline (sample locations indicated by white triangles in Figure 6a).

during the past two decades [*Carr et al.*, 2013]. Summer (JJA) air temperatures showed a similar warming trend of 0.20°C per year ($R^2 = 0.68$) between 1990 and 2010, which was particularly marked from 1996 onwards (Figure 4b). The number of PDDs at Kitsissorsuit were very high in 1995 and then showed a strong positive trend between 1996 and 2001, followed by a further period of warming between 2004 and 2009 (Figure 4b).

[23] Mean summer (JJA) and autumn (SON) sea ice concentrations showed a decreasing trend from 1997 to 2004 and then increased between 2004 and 2007, before declining once more from 2007 to 2009 (Figure 4c). The glacier fjords became seasonally ice free during the summers of 2000 to 2003, 2005 and 2009, with the number of ice free months peaking in 2001, 2003, and 2009 (Figure 4d). MODIS SST data show warming between 2000 and 2002,

followed by cooling of approximately 1°C between 2002 and 2008 (Figure 4e). SSTs then increased by 1.5°C between 2009 and 2010. The Reynolds SST data show no net trend between 1990 and 1995, followed by warming of almost 2°C between 1996 and 1999. SSTs cooled gradually until 2005 and then warmed between 2008 and 2010 (Figure 4e). The two SST data sets follow a similar overall pattern, but the MODIS values are consistently cooler than the Reynolds data (Figure 4e).

4. Discussion

[24] All glaciers underwent net retreat during the study period, but despite comparable glacier sizes and forcing, the magnitude, pattern, and rate of retreat varied dramatically between individual glaciers (Table 1, Figures 1 and 4). We first discuss glacier response to atmospheric and oceanic forcing at seasonal timescales, in order to investigate the factors influencing calving rates and net frontal position, and then consider these relationships at interannual to decadal timescales, before assessing the role of glacier-specific factors.

4.1. Influence of Atmospheric and Oceanic Forcing on Seasonal Glacier Behavior

4.1.1. Alison Glacier

[25] Between 2004 and 2007, seasonal variations in frontal position at AG corresponded closely to changes in sea ice concentrations within the glacier fjord at the start and the end of the calving season (Figure 3a). This is exemplified by its behavior in 2005, when summer sea ice concentrations were particularly low and the transition between fast ice and ice free conditions was particularly rapid (Figure 3a). Seasonal retreat began from 26 June 2005, coincident with sea ice reducing from 100% to 10% between 20 June and 4 July (Figure 3a). Conversely, sea ice concentrations reached 100% by 21 November 2005, which was rapidly followed by the onset of winter advance from 29 November 2005 (Figure 3a).

[26] The onset of seasonal retreat/advance shows a similar coincidence with sea ice loss/formation during each calving season between 2004 and 2007 (Figure 3a), suggesting that sea ice may be a primary control on seasonal frontal position variations at AG during this period. This is supported by comparison of ice velocities and terminus advance rates for winter 2005–2006 (Table 1), which suggest that the calving front advanced at approximately 95% of the glacier flow speed and that winter calving was therefore minimal. These results agree with findings from elsewhere on the GrIS, which suggest that sea ice may suppress winter calving rates by up to a factor of six by forming a weak seasonal ice shelf, or mélange, which inhibits calving from the terminus [*Amundson et al*., 2010; *Joughin et al*., 2008b; *Sohn et al*., 1998]. In contrast, spring-time disintegration of the mélange may promote retreat by allowing high summer calving rates to commence [*Ahn and Box*, 2010; *Amundson et al*., 2010; *Howat et al*., 2010; *Joughin et al*., 2008b]. Thus, sea ice is likely to be an important control on the frontal position and calving rate of AG at seasonal timescales.

[27] The onset of seasonal retreat at AG also partially coincided with the seasonal increase in air temperatures to above 0°C, although with a delay of approximately three to four weeks (Figure 3b). In spring 2005, for example, SATs first exceeded 0°C on 17 May, prior to terminus retreat on 26 June (Figure 3b). In general, air temperatures at AG rose above 0°C between mid-May and mid-June and glacier retreat began in late June (Figure 3b). The seasonal increase in air temperatures could promote retreat via a number of mechanisms [*Carr et al*., 2013], including: (i) meltwater enhanced crevassing at the glacier terminus [*Andersen et al*., 2010; *Sohn et al*., 1998; *Vieli and Nick*, 2011]; (ii) melting of sea ice/ice mélange; and (iii) enhancement of submarine melt rates by subglacial plume flow [*Motyka et al*., 2003; *Motyka et al*., 2011; *Straneo et al*., 2011]. The lack of available data precludes investigation of the latter mechanism, but the first two processes are supported by the presence of numerous water-filled crevasses and supraglacial lakes close to AG's terminus during summer, as observed from satellite imagery (Figure 1), and by the strong correlation between SATs and sea ice ($r = 0.72$). At the end of the calving season, air temperatures at AG fall below freezing approximately 1.5 to 2.5 months before the onset of winter advance (Figure 3b). This is exemplified by winter June 2005/2006, when air temperatures were below freezing by 18 September, but seasonal retreat persisted until 29 November (Figure 3b). These observations suggest that air temperatures may contribute to seasonal retreat at AG, but their influence on seasonal advance may be limited, which is consistent with previous findings from Jakobshavn Isbrae (JI), west Greenland [*Sohn et al*., 1998].

[28] Between 2004 and 2007, SST warming from June onwards was coincident with the onset of seasonal retreat at AG (Figure 3c). However, the most rapid retreat did not coincide with peak SSTs: in 2005, for example, the warmest SSTs occurred in August, yet the glacier front advanced slightly between 6 and 29 August (Figure 3c). Similarly, in 2006, peak SSTs in July and August were coincident with a small terminus advance between 23 July and 5 September (Figure 3c). This suggests that the frontal position responds to SST warming, as opposed to peak SSTs, which may result from the relationship between SSTs and sea ice concentrations. SST warming early in the season would melt sea ice at the glacier terminus and could thus promote retreat, given the apparent sensitivity of AG to sea ice concentrations. In contrast, peak SSTs would have a lesser affect, as sea ice has largely melted by this point in the season (Figure 3a). This mechanism is supported by the moderate correlation between SSTs and sea ice at AG ($r = 0.52$) and the coincidence of SST warming with the seasonal disintegration of fast ice (i.e., 100%) at the glacier front (Figure 3). The limited correspondence between peak SSTs and retreat rates also suggests that undercutting at the waterline [*Benn et al*., 2007; *Vieli et al*., 2002] due to SST warming is not a primary driver of retreat.

[29] At present, subsurface oceanographic data are not available from AG's fjord, and the only data available for the region are model outputs from the Hadley Centre EN3 quality controlled subsurface ocean temperature and salinity data set [*Ingleby and Huddleston*, 2007]. As noted, these data only provide information on water temperature on the continental shelf and are therefore unlikely to be representative of conditions at the glacier front. However, the modeled depth profile sampled from the continental shelf, immediately offshore of the study region, suggests that warm water is

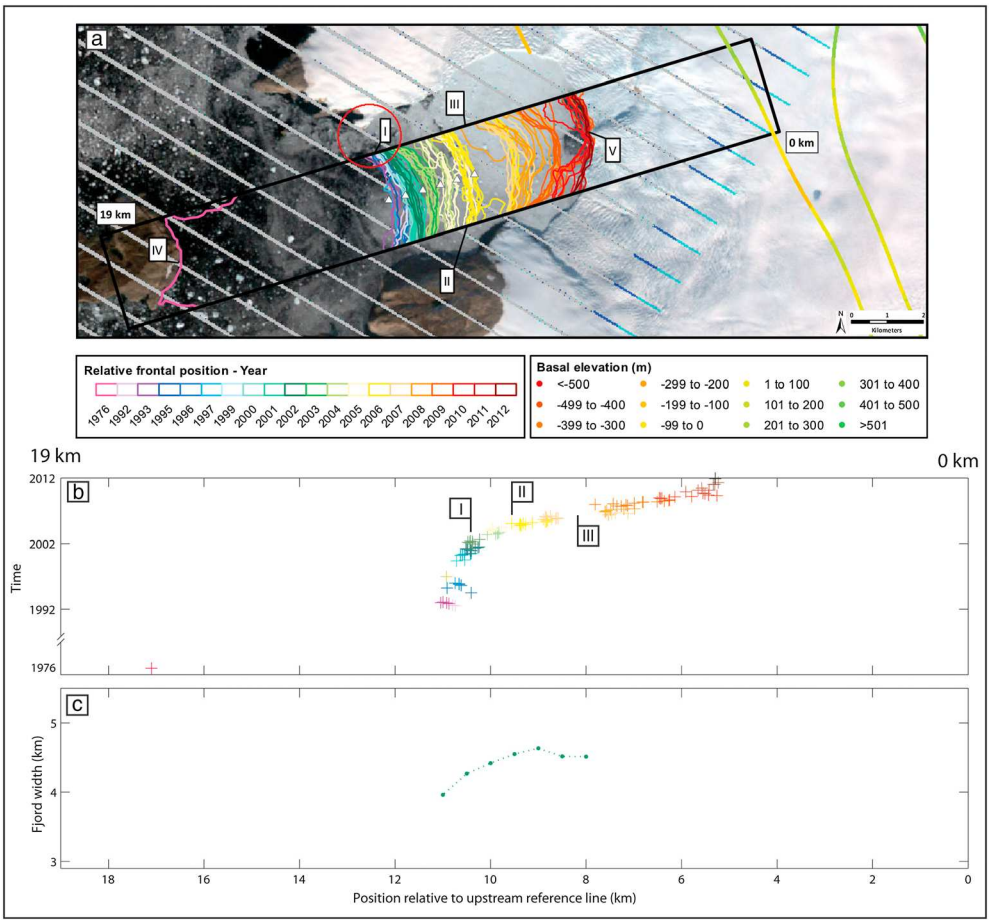

Figure 7. Mean annual ocean temperature profile from Hadley Center EN3 reanalysis data. Profiles area color coded according to year.

present at depth (~100 to 150 m) and underlies cooler surface water (Figure 7). This profile is consistent with empirical data from central-west Greenland [*Holland et al.*, 2008], and previous studies have shown that warm Atlantic Water can access Greenland outlet glacier fjords from the continental shelf at depth [*Christoffersen et al.*, 2011; *Holland and Thomas*, 2008; *Johnson et al.*, 2011; *Mayer et al.*, 2000; *Straneo et al.*, 2011; *Straneo et al.*, 2010]. Given that high summer submarine melt rates have been linked to seasonal mass loss in central-west Greenland [*Rignot et al.*, 2010], it is possible that similar processes may influence seasonal glacier behavior at AG. This is supported by estimated submarine melt rates of 0.26 m d^{-1} at AG, which may account for a significant portion of ice volume loss {Enderlin, 2013 #379}. However, the current lack of data from within the fjord precludes a more detailed assessment of this potential control on seasonal behavior. It is clear therefore, that there is an urgent need for subsurface measurements of ocean temperature at AG and other Greenland outlet glacier fjords. Such data are required for numerical models that incorporate oceanic forcing and would also allow a more detailed assessment of the influence of meltwater plumes on submarine melt rates: subglacial discharge may increase melting by forming a plume of cool, buoyant water at the terminus and promoting a compensatory inflow of warmer ocean water at depth [*Motyka et al.*, 2003; *Motyka et al.*, 2011; *Straneo et al.*, 2011]. This interaction is currently poorly understood [*Straneo et al.*, 2011], but may be significant at AG, given the very dramatic warming observed during the past two decades (Figure 4b).

[30] In summary, we suggest that seasonal retreat at AG may be initiated by a combination of spring-time sea ice loss and meltwater-enhanced crevassing. Winter sea ice formation may slow calving rates and promote seasonal advance and air temperatures and SSTs may indirectly influence frontal position, via their relationship with sea ice concentrations. These results indicate that multiple atmospheric and oceanic forcing factors influence seasonal frontal position variations at AG, but that their relative contribution varies during the year.

4.1.2. Additional Study Glaciers

[31] In contrast to the close correspondence observed at AG, the relationship between sea ice and glacier frontal position is less apparent on the other study glaciers. NW1 and IGD show a pattern of response to seasonal forcing that was representative of the other glaciers within the study region (Figure 3, see auxiliary materials). At both glaciers, the onset of seasonal retreat and advance sometimes coincided with sea ice clearance and re-formation, respectively, but it also predated it on a number of occasions and instead often showed a closer correspondence to periods when air temperatures rose above freezing. At NW1, for example, retreat began between 6 and 31 May 2005, which significantly

predated sea ice clearance between 20 June and 4 July (Figure 3d) and coincided with air temperatures rising above freezing on 17 May in 2005 (Figure 3e). Similarly, IGD retreated between 14 April and 28 June 2009, but sea ice clearance did not occur until 22 June – 7 July (Figure 3g).

[32] Although the onset of winter advance at NW1 and IGD was generally concurrent with winter sea ice formation and occurred substantially after air temperatures fell below zero (Figure 3), this was not always the case. In winter 2009, for example, terminus advance began at both glaciers between 31 August and 8 October and therefore predated winter sea ice formation between 23 November and 7 December (Figures 3d and 3g). Furthermore, comparison of winter advance rates and ice velocities (Table 1) indicates that calving does not cease entirely at IGD, suggesting that winter sea ice formation may exert a weaker influence on seasonal glacier advance than at AG. In contrast to AG, the onset of seasonal retreat at NW1 and IGD frequently preceded SST warming (Figures 3f and 3i). This differing response may reflect the weaker influence of sea ice at NW1 and IGD, which may reduce the contribution of SSTs to frontal retreat via sea ice melt.

[33] These observations indicate that seasonal frontal position variations at NW1, IGD, and the other study glaciers are influenced by both air temperatures and sea ice. However, sea ice concentrations and SSTs may be a less significant control than at AG, suggesting that glacier-specific factors may be modulating the response to seasonal forcing. In contrast to the other study glaciers, AG initially terminated in a floating ice tongue, and a number of lines of evidence suggest that this tongue was near to floatation between 2004 and 2007. First, it calved several large, tabular icebergs (Figure 2), which are only thought to occur from floating termini [*Amundson et al*., 2010]. Second, the tabular icebergs often calved back to large rifts (Figure 2), which are associated with near-floating ice [*Joughin et al*., 2008a]. Third, the tongue's surface elevation profile was very flat [*McFadden et al*., 2011]. The presence of a floating ice tongue may account for AG's greater sensitivity to seasonal sea ice forcing, and hence to SSTs, as basal shear stresses would be low over areas close to floatation, meaning that the relative contribution of longitudinal stresses to the force balance would increase [*Echelmeyer et al*., 1994] and that variations in longitudinal stresses associated with changes in sea ice buttressing may have had a greater influence on retreat rates. This is supported by AG's behavior subsequent to 2007, when evidence suggests that the terminus began to reground and the correspondence between seasonal sea ice disintegration and the onset of retreat became less pronounced, with retreat predating sea ice clearance in 2009 (Figure 3a). These results suggest that the seasonal response of the study glaciers to atmospheric and oceanic forcing varies according to terminus type and that this relationship may change as the glacier terminus evolves during retreat.

4.2. Interannual Glacier Behavior and Atmospheric and Oceanic Controls

[34] All glaciers in the study area retreated between 1993 and 2010 (Figures 1 and 4), coincident with declining summer (JJA) and autumn (SON) sea ice concentrations and a dramatic air temperature increase of almost 8°C (Figure 4). Given the influence of sea ice and air temperatures on seasonal glacier behavior within the study region, we suggest that these factors are likely to also be primary controls at interannual timescales, via their influence on net frontal position and calving rates.

[35] At AG, retreat followed increased air temperatures and sea ice decline, with peak retreat rates occurring within one year of minimum sea ice concentrations in 2003 (Figure 4). Seasonal results suggest that sea ice is a key control on the timing of retreat/advance at AG (Figure 3a) and so early disintegration/late formation of sea ice may have triggered net terminus retreat by extending the duration of seasonally high summer calving rates, as proposed for other Greenland outlet glaciers [e.g., *Howat et al*., 2010; *Joughin et al*., 2008b]. This is consistent with the pattern of interannual retreat at AG (Figure 4a), where very large seasonal retreats in 2004 and 2005, totaling almost 6 km, followed a prolonged decline in sea ice concentrations and substantial increase in the duration of ice free conditions (Figure 3a). The very strong increase in air temperatures may also have contributed to net retreat at AG, potentially via meltwater enhanced crevassing at the terminus [*Sohn et al*., 1998; *Vieli and Nick*, 2011], increased sea ice melting and/or enhanced submarine melt rates due to increased subglacial discharge. These observations are in agreement with previous results from the Uummannaq region of west Greenland [*Howat et al*., 2010] and JI [*Joughin et al*., 2008b; *Vieli and Nick*, 2011], which suggest that extension of the seasonal calving cycle through reduced sea ice concentrations and/or increased air temperatures may be sufficient to trigger rapid interannual retreat.

[36] Output from the EN3 model indicates that ocean temperatures at depth increased substantially between 1998 and 1999 at the continental shelf (Figure 7), which is broadly consistent with the sudden increase in subsurface ocean temperatures recorded on the central-west Greenland continental shelf between 1997 and 1998 {Holland, 2008 #41}. However, the modeled warming substantially predates the onset retreat at AG (Figure 4). Moreover, estimated melt rates at AG showed no clear trend between 2002 and 2007 {Enderlin, 2013 #379}, whereas glacier retreat rates varied dramatically during this period (Figure 4a). This is consistent with previous results, which found no statistically significant relationship between estimated melt rate and either glacier retreat or velocity at AG {Enderlin, 2013 #379}. The very limited available evidence shows no clear relationship between subsurface oceanic warming, submarine melt rates, and glacier retreat at AG. However, very little information is available, and detailed subsurface oceanographic measurements from within the fjord would be required to investigate the potential influence of subsurface ocean warming on AG.

[37] The MODIS and Reynolds SST data follow a similar interannual pattern (Figure 4), although MODIS values are consistently cooler than the Reynolds data set. We attribute this difference to the greater spatial resolution of the MODIS data, which allows SSTs to be sampled closer to the glacier termini. Consequently, glacial meltwater discharge and icebergs from the termini would have a greater influence on the MODIS SSTs and would thus give cooler values. The MODIS data indicate that SSTs warmed by 1°C between 2000 and 2002, which was coincident with the onset of retreat at AG, low summer sea ice concentrations

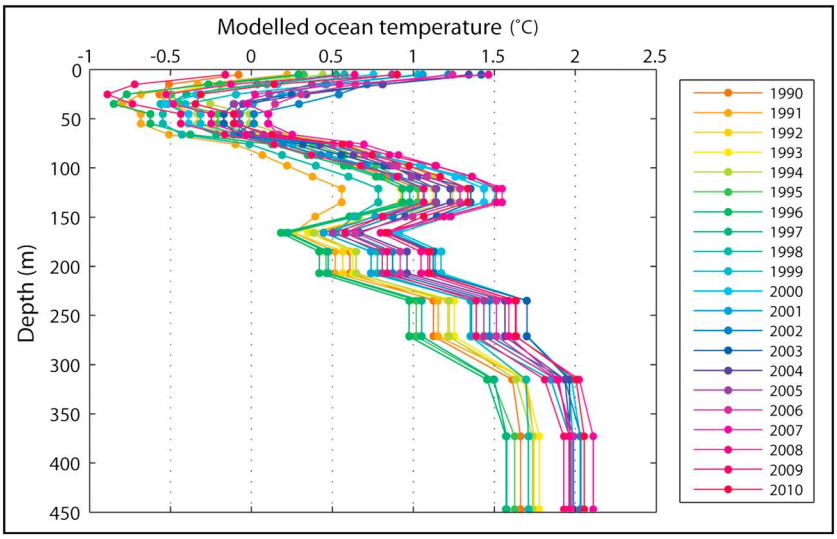

Figure 8. Frontal position of NW1 in relation to basal elevation and fjord width parallel to the glacier terminus. (a) NW1 frontal position over time (colored lines) in relation to ice-bottom elevations from CReSIS radar depth sounder flightlines, color coded from green (high elevation) to red (low elevation). Labeled positions are discussed in the text. Base image: Landsat scene acquired 11 September 2011 and provided by USGS GLOVIS. (b) NW1 frontal position over time (colored crosses), relative to upstream reference line. (c) Fjord width perpendicular to the cent**er**line at 500 m intervals from the upstream reference line (sample locations indicated by white triangles in a).

and an extended duration of ice-free conditions (Figure 4). Based on relationships observed at seasonal timescales, warmer SSTs may have initiated retreat by causing early sea ice loss and thus extending the duration of high summer calving rates. However, the MODIS data then show a cooling between 2002 and 2008 and the Reynolds data demonstrate little trend during this period, despite AG continuing to retreat rapidly (Figure 4). Furthermore, significant SST warming occurred in 1996–1999 and 2008–2010, yet the front exhibited little change. This suggests that AG's response to SST changes is nonlinear, so that the magnitude of retreat does not depend only on the magnitude of forcing. A similar nonlinearity is evident in the relationship with sea ice and air temperature trends. This was particularly notable in 2009 when sea ice concentrations and duration were comparable to 2001 and JJA SATs and PDDs reached their maximum for the study period, yet retreat rates remained low (Figure 4). Together, this evidence indicates that the response of AG to these potential controls was modulated by glacier-specific factors.

[38] Interannual retreat of the other study glaciers was also coincident with sea ice decline and atmospheric warming (Figure 4), which is consistent with controls operating at seasonal timescales. However, despite being subject to very similar forcing, the magnitude and rate of retreat differed dramatically between individual glaciers (Table 1, Figures 1 and 4). These results agree with previous findings from western Greenland, which found no consistent relationship between marine-terminating outlet glacier behavior and atmospheric or oceanic forcing [*McFadden et al.*, 2011]. Furthermore, the pattern of retreat varied markedly across the study region: net retreat at AG and NW1 largely occurred via very large seasonal retreats with limited seasonal readvance (Figures 3a, 3d, and 4a), whereas the other glaciers retreated more gradually, with limited variation in the magnitude of seasonal frontal position variations (Figures 3g and 4a). This contrasting behavior suggests that the study glaciers reacted very differently to external forcing and that factors specific to each glacier are a key determinate of their response.

[39] On the majority of the study glaciers, retreat rates were substantially higher during the past decade than between 1976 and 2001 (Table 1 and Figures 5 and 6), and this is consistent with a previous study which identified a large episode of mass loss in northwest Greenland between 2005 and 2010 [*Kjær et al.*, 2012]. It has also been proposed that northwest Greenland underwent an earlier event between 1985 and 1993, during which dynamic mass loss exceeded that between 2005 and 2010. Furthermore, AG was highlighted as an area of rapid thinning between 1985 and 2005 [*Kjær et al.*, 2012]. Our results suggest that majority of the study glaciers showed limited net retreat between 1976 and 2001 (Table 1 and Figure 6), and AG in particular showed very little change during this period (Figure 5 and Table 1). This contrasts dramatically with observed retreat rates of almost 2.5 km a^{-1} between 2001 and 2005 at AG (Figure 5). We therefore suggest that the observed thinning at AG between 1985 and 2005 was a response to rapid retreat and loss of the floating tongue between 2001 and 2005, as opposed to an earlier mass loss event. Furthermore, we highlight recent retreat rates at AG as exceptional since at least 1976. Our data record substantial retreats on NW1 and NW2 (Figure 8 and Table 1), but the vast majority of these changes occurred prior to 1986 and therefore predate the proposed dynamic event. At NW7, retreat largely occurred on the western portion of the terminus and was coincident with the loss of a section of ice adjoining the lateral margin of the glacier. We therefore suggest that retreat at NW7 was a response to the reduction in buttressing associated with this ice loss, as opposed to a

direct dynamic response to changes in atmospheric or oceanic forcing at its terminus. Consequently, we do not observe substantial and widespread changes in frontal position within our study region at the time of the proposed discharge event.

4.3. Role of Glacier-Specific Factors

[40] We examined retreat rates in relation to a number of glacier-specific factors, including initial glacier width, ice velocity, bed topography, fjord geometry, and terminus type. We found no statistically significant relationship between the mean glacier retreat rate for 1993 to 2010 and either initial glacier terminus width in January 1993 ($r = -0.085$) or with initial ice velocity in winter 2000–2001 ($r = -0.080$). However, our results suggest that along-flow variations in fjord width may play an important role in ice dynamics within the study region, via their influence on lateral stresses.

[41] The pattern of retreat at AG suggests that along-flow variations in fjord width and potentially basal pinning points may be important controls on retreat. Peak retreat rates immediately followed terminus recession into a comparatively wide section of its fjord from July 2004 onwards (Figure 5; Point I) and persisted until the calving front reached a lateral constriction in late August 2005 (Figure 5; Point II). At this point, retreat slowed dramatically, and the terminus position remained comparatively stable until July 2010. Narrowing of the glacier fjord may have temporarily slowed retreat via two mechanisms [*Jamieson et al*., 2012]: (i) due to the principle of mass conservation, the glacier needs to thicken and the surface slope to steepen in order to maintain the same ice flux, which would reduce thinning rates and the vulnerability of the ice to full thickness fracture, thus decreasing calving rates and slowing retreat [*O'Neel et al*., 2005]; and (ii) lateral stresses tend to increase with reducing width [*Raymond*, 1996], thus increasing resistance to flow and promoting deceleration, thickening, and slower retreat. Furthermore, a number of lines of evidence suggest that AG's terminus began to ground at this point: (i) the substantial reduction in the magnitude of seasonal frontal position variation, particularly seasonal retreat, from winter 2005 onwards (Figure 3A), (ii) the change in calving style from tabular to capsizing icebergs, (iii) the increased occurrence of glacial earthquakes, which are associated with grounded termini [*Veitch and Nettles*, 2012], and (iv) the development of a steeper surface profile near the terminus from 2006 onwards [*McFadden et al*., 2011]. Although grounding is unconfirmed, it may have produced further positive feedbacks between glacier thickening, increased basal stresses and reduced frontal retreat rates [*Schoof*, 2007; *Vieli et al*., 2001].

[42] Based on these observations, we suggest that the comparative stability of AG's floating tongue between 1976 and 2001 (Figure 5; Point III) was also facilitated by the relatively narrow width of the fjord and/or the presence of basal pinning points. Although fjord bathymetry data are currently unavailable, a bedrock island and a possible ice rumple are apparent at the northern margin of AG (Figure 5; Inset 1). Terminus retreat past this feature and into a wider section of the fjord immediately preceded the first phase of rapid retreat at AG (Figure 5: Point IV), providing empirical support for the contribution of basal and lateral pinning points to the comparative stability of AG's terminus between 1976 and 2001. These findings agree with empirical results from southern Greenland, which highlighted the role of fjord topography, particularly lateral pinning points, in determining glacier frontal position and modulating glacier response to climatic forcing [*Warren and Glasser*, 1992] and with recent numerical modeling studies, which have highlighted the influence of variations in trough width on ice stream retreat [*Jamieson et al*., 2012]. The presence of a floating tongue at AG may have further contributed to its rapid retreat, as it would be vulnerable to basal crevassing [*van der Veen*, 1998] and positive feedbacks associated with dynamic thinning, once the glacier had been dislodged from its lateral/basal pinning points [*Meier and Post*, 1987; *Schoof*, 2007; *Vieli and Nick*, 2011].].

[43] Our data suggest that width may also have influenced the rate and pattern of retreat at NW1. The glacier occupied a fairly constant position between 1992 and 2001 and retreat rates were low ($24.8\ m\ a^{-1}$) (Figure 8; Point I). During this period, the terminus was located in a relatively narrow section of the fjord, and the northern margin was in contact with a lateral pinning point (Figure 8; Point I), which together would promote slower retreat. Retreat rates then increased substantially as the glacier front moved through a wider section of fjord between June 2001 and July 2006 (Figure 8; Point II), as observed at AG. NW1 underwent the most rapid retreat of the study period between 3 July and 9 September 2006, when the central portion of the front retreated inland of the rock islands that had previously bounded the terminus, which would have significantly reduced lateral stresses and promoted dynamic thinning and retreat [*Jamieson et al*., 2012; *O'Neel et al*., 2005; *Raymond*, 1996]. The central section continued to retreat rapidly and formed a large, concave bay by the end of the study period (Figure 8). The influence of the islands on the frontal position of NW1 is further supported by its earlier behavior: in 1976, NW1 terminated on a rock island (Figure 8; Point IV) and then retreated by 6 km by 1986, at which point the terminus reached the narrow section between the rock islands (Figure 8; Point I). Although the exact timing and pattern of retreat are unknown, this suggests that the front may have retreated rapidly after losing contact with the outer island. The most recent data from NW1 show that retreat has slowed (Figure 8) and the retreat pattern indicates that the terminus may have reached a basal pinning point and/or shallower section (Figure 8; Point V), although bathymetric data would be needed to confirm whether this is the case.

[44] The termini of most of the other study glaciers were bounded laterally by rock islands, as at NW1, but they did not retreat beyond these lateral constraints during the study period (Figure 1). The exception to this was IGD, which had a similar fjord configuration to AG (Figure 1). However, IGD's terminus occupied a relatively narrow section of fjord for the majority of the study period (Figure 6; Inset; Point I). The variation in fjord width in the along-flow direction was much less at IGD (10%) than at AG (17%), within the section over which the termini retreated (Figures 5 and 6), and this would limit the contribution of variations in lateral stresses to retreat. On the basis of these observations, we suggest that differences in lateral topography may largely account for the high retreat rates observed at AG and NW1 and for their differing dynamic response to atmospheric and oceanic forcing. The lateral/basal topography at AG and NW1

implies that even a comparatively small additional seasonal retreat, in response to external forcing, may be sufficient to move the termini into a position where rapid retreat can occur via a series of positive feedbacks. In contrast, the other study glaciers did not retreat beyond the confines of their bounding islands and/or undergo significant changes in fjord width, thus minimizing variations in resistive stresses during retreat. Consequently, sea ice decline and/or atmospheric warming may not yet be sufficient to initiate rapid retreat on the majority of the study glacier termini.

4.4. Summary and Future Outlook

[45] Our results suggest that the response of individual glaciers to atmospheric and oceanic forcing is substantially modulated by variations in fjord width, terminus type, and, potentially, basal pinning points. Based on the observed relationships, the following factors are likely to predispose outlet glaciers to rapid retreat: the loss of contact with lateral/basal pinning points; significant widening of the fjord during retreat; and/or the presence of a floating ice tongue. Our findings are in accordance with previous results from western Greenland, which found no consistent relationship between glacier retreat and initial glacier width [*McFadden et al*., 2011]. However, in contrast to *McFadden et al*. [2011], who used a single measurement of glacier width prior to the onset of retreat, our data suggest that even subtle variations in the along-flow width of the constraining fjord may be a primary controlling factor on glacier retreat rates, once retreat has been initiated [c.f. *Jamieson et al*., 2012].

[46] The role of fjord geometry may be particularly significant in the near future in the study region, as data suggest that IGD and AG may be close to retreating inland of their fjords and into areas of comparatively deep basal topography (Figures 5 and 6). This is supported by the most recent data from AG, which show that its northern margin retreated by 2.3 km between July 2010 and September 2011 (Figure 5; Point V) but then halted at another lateral constriction, formed by a rock outcrop (Figure 5; Point VI and Inset 2), where it remained until the last-available image in May 2012. This suggests that the lateral pinning point may have temporarily halted retreat and highlights the potentially strong influence of variations in fjord width on the pattern of retreat at AG. Importantly, no further lateral constrictions are visible at the northern margin of AG and the ice flow appears to diverge markedly upglacier (Figure 5). Basal data suggest that the area inland of the current terminus is up to 700 m deep (Figure 5). This deeper area may initially facilitate rapid retreat via buoyancy-driven feedbacks [e.g., *Joughin et al*., 2008b; *Vieli and Nick*, 2011], once the terminus ice has thinned sufficiently to remove it from its current lateral pinning point. However, the basal topography becomes shallower approximately 6 km inland and may therefore eventually promote slower retreat.

[47] Following decades of minimal variation in terminus position, IGD began to retreat in winter 2008 and may also be close to moving inland of the lateral margins of its fjord (Figure 6; Inset; Point II). Bed depths inland of the present terminus reach up to 600 m and the combined effects of the terminus moving beyond the constraints of its fjord and into an area of deep topography could facilitate rapid retreat. However, two channels of up to 800 m depth begin approximately 7 km inland of the front (Figure 6). Dependent on their detailed geometry, these channels could promote lower retreat rates, once the terminus retreats into them, by constraining flow and increasing resistive stresses. The other glaciers within the study region currently terminate on a series of rock outcrops (Figure 1). Based on observations from NW1, these glaciers may also begin to retreat rapidly if future atmospheric and oceanic forcing is sufficient to force the termini beyond the constraining influence of these islands.

5. Conclusions

[48] Our results suggest that marine-terminating outlet glacier behavior is influenced by a combination of atmospheric, oceanic, and glacier-specific controls within the study region. At seasonal timescales, sea ice and air temperatures appear to be the primary external controls on frontal position. The response to seasonal forcing varies between study glaciers and can evolve during retreat, with AG showing a greater sensitivity to sea ice when its floating tongue existed. All of the study glaciers underwent net retreat between 1993 and 2010, coincident with marked sea ice decline and almost 8°C of atmospheric warming. Retreat at AG reached rates of almost 2.5 km a^{-1} between 2001 and 2005, prior to which the terminus had occupied a very similar position since at least 1976. The magnitude, rate, and pattern of retreat varied substantially between individual glaciers, with retreat rates at AG and NW1 far exceeding the regional average. This suggests that glacier-specific factors play an important role in determining outlet glacier response to external forcing, and we identify variations in fjord width and terminus type as key factors. Fjord geometry may be a key control on the near-future evolution of AG and IGD, as both glaciers are close to retreating beyond the confining influence of their fjord margins and the inland basal topography may significantly influence their future pattern of retreat. We highlight the need for very high temporal resolution data and in situ measurements, particularly of fjord water conditions, in order to fully understand the relative importance of each forcing factor and the role of feedbacks such as plume-enhanced submarine melting. Furthermore, high-resolution information on subglacial topography and fjord bathymetry is needed to further assess the influence of fjord geometry on outlet glacier behavior. Our results underscore the importance of glacier-specific factors in determining the response of marine-terminating outlet glaciers to atmospheric and oceanic forcing, and we highlight the need to consider these factors when interpreting outlet glacier retreat rates and forecasting future behavior.

[49] **Acknowledgments.** This work was supported by a Durham Doctoral Studentship, granted to J.R. Carr. Envisat and ERS Image Mode Precision scenes were provided by the European Space Agency (ESA). We acknowledge the use of data and/or data products from CReSIS generated with support from NSF grant ANT-0424589 and NASA grant NNX10AT68G. We thank T. Benham, A. Luckman, D. Small, and I. Joughin for their helpful comments, and three anonymous reviewers.

References

Ahn, Y., and J. E. Box (2010), Glacier velocities from time-lapse photos: Technique development and first results from the Extreme Ice Survey (EIS) in Greenland, *J. Glaciol.*, *198*, 723–734.

Alley, R. B. (1991), Sedimentary processes may cause fluctuations of tidewater glaciers, *Ann. Glaciol.*, *15*, 119–124.

Amundson, J. M., M. Fahnestock, M. Truffer, J. Brown, M. P. Lűthi, and R. J. Motyka (2010), Ice mélange dynamics and implications for terminus stability, Jakobshavn Isbræ, Greenland, *J. Geophys. Res.*, *115*, F01005, doi:10.1029/2009JF001405.

Andersen, M. L., et al. (2010), Spatial and temporal melt variability at Helheim Glacier, East Greenland, and its effect on ice dynamics, *J. Geophys. Res.*, *115*, F04041, doi:10.1029/2010JF001760.

Benn, D. I., C. R. Warren, and R. H. Mottram (2007), Calving processes and the dynamics of calving glaciers, *Earth Sci. Rev.*, *82*, 143–179.

Bevan, S. L., A. J. Luckman, and T. Murray (2012), Glacier dynamics over the last quarter of a century at Helheim, Kangerdlugssuaq and 14 other major Greenland outlet glaciers, *Cryosphere*, *6*, 923–937.

Cappelen, J. (2011), DMI monthly climate data collection 1768-2010, Denmark, the Faroe Islands and Greenland, *Tech. Rep*., 11-05, Dan. Meteorol. Inst., Copenhagen.

Carr, J. R., C. R. Stokes, and A. Vieli (2013), Recent progress in understanding marine-terminating Arctic outlet glacier response to climatic and oceanic forcing: Twenty years of rapid change, *Progress in Physical Geography*, doi:10.1177/0309133313483163.

Carstensen, L. S., and B. V. Jørgensen (2011), Weather and cliamte data from Greenland 1958-2010, *Tech. Rep.*, *11-10*, Danish Meteorological Institute (DMI), Denmark.

Christoffersen, P., R. Mugford, K. J. Heywood, I. Joughin, J. Dowdeswell, J. P. M. Syvitski, A. Luckman, and T. J. Benham (2011), Warming of waters in an East Greenland fjord prior to glacier retreat: Mechanisms and connection to large-scale atmospheric conditions, *Cryosphere Discuss.*, *5*, 1335–1364.

Echelmeyer, K. A., W. D. Harrison, C. Larsen, and J. E. Mitchell (1994), The role of the margins in the dynamics of an active ice stream, *J. Glaciol.*, *40*(136), 527–538.

Enderlin, E. M., and I. M. Howat (2013), Submarine melt rate estimates for floating termini of Greenland outlet glaciers (2000–2010), *J. Glaciol.*, *59*(213), pp. 67–75(9).

Holland, D. M., R. H. Thomas, B. de Young, M. H. Ribergaard, and B. Lyberth (2008), Acceleration of Jakobshavn Isbræ triggered by warm subsurface ocean waters, *Nat. Geosci.*, *1*, 1–6.

Howat, I. M., and A. Eddy (2011), Multi-decadal retreat of Greenland's marine-terminating glaciers, *J. Glaciol.*, *57*(203), 389–396.

Howat, I. M., I. Joughin, M. Fahnestock, B. E. Smith, and T. Scambos (2008), Synchronous retreat and acceleration of southeast Greenland outlet glaciers 2000-2006; Ice dynamics and coupling to climate, *J. Glaciol.*, *54*(187), 1–14.

Howat, I. M., J. E. Box, Y. Ahn, A. Herrington, and E. M. McFadden (2010), Seasonal variability in the dynamics of marine-terminating outlet glaciers in Greenland, *J. Glaciol.*, *56*(198), 601–613.

Howat, I. M., Y. Ahn, I. Joughin, M. van den Broeke, J. Lenaerts, and B. Smith (2011), Mass balance of Greenland's three largest outlet glaciers, 2000–2010, *Geophys. Res. Lett.*, *38*, L12501, doi:10.1029/2011GL047565.

Ingleby, B., and M. Huddleston (2007), Quality control of ocean temperature and salinity profiles - historical and real-time data, *J. Mar. Syst.*, *65*, 158–175, doi:10.1016/j.jmarsys.2005.11.019.

Intergovernmental Panel on Climate Change (2007), *The Physical Science Basis. Contribution of Working Group I to the Fourth Assessment Report of the Intergovernmental Panel on Climate Change*, Cambridge Univ. Press, Cambridge, U. K.

Jacob, T., J. Wahr, W. T. Pfeffer, and S. Swenson (2012), Recent contributions of glaciers and ice caps to sea level rise, *Nature*, *482*, 514–518.

Jamieson, S. S. R., A. Vieli, S. J. Livingstone, C. Ó Cofaigh, C. R. Stokes, C.-D. Hillenbrand, and J. A. Dowdeswell (2012), Ice stream stability on a reverse bed slope, *Nat. Geosci.*, *5*, 799–802.

Johnson, H. L., A. Münchow, K. K. Falkner, and H. Melling (2011), Ocean circulation and properties in Petermann Fjord, Greenland, *J. Geophys. Res.*, *116*, C01003, doi:10.1029/2010JC006519.

Joughin, I., I. M. Howat, R. B. Alley, G. Ekström, M. Fahnestock, T. Moon, M. Nettles, M. Truffer, and V. C. Tsai (2008a), Ice-front variation and tidewater behaviour on Helheim and Kangerdlugssuaq Glaciers, Greenland, *J. Geophys. Res.*, *113*, F01004, doi:10.1029/2007JF000837.

Joughin, I., I. M. Howat, M. Fahnestock, B. Smith, W. Krabill, R. B. Alley, H. Stern, and M. Truffer. (2008b), Continued evolution of Jakobshavn Isbrae following its rapid speedup, *J. Geophys. Res.*, *113*, F04006, doi:10.1029/2008JF001023.

Joughin, I., B. Smith, I. M. Howat, T. Scambos, and T. Moon (2010a), Greenland flow variability from ice-sheet-wide velocity mapping, *J. Glaciol.*, *56*(197), 415–430.

Joughin, I., B. E. Smith, I. Howat, and T. Scambos (2010b), *MEaSUREs Greenland Ice Sheet velocity map from InSAR data*, http://nsidc.org/data/docs/measures/nsidc0478_joughin/, Natl. Snow and Ice Data Cent., Boulder, Colo.

Joughin, I., B. E. Smith, I. M. Howat, D. Floricioiu, R. B. Alley, M. Truffer, and M. Fahnestock (2012), Seasonal to decadal scale variations in the surface velocity of Jakobshavn Isbrae, Greenland: Observation and model-based analysis, *J. Geophys. Res.*, *117*, F02030, doi:10.1029/2011JF002110.

Khan, S. A., J. Wahr, M. Bevis, I. Velicogna, and E. Kendrick (2010), Spread of ice mass loss into northwest Greenland observed by GRACE and GPS, *Geophys. Res. Lett.*, *37*, L06501, doi:10.1029/2010GL042460.

Kjær, K. H., et al. (2012), Aerial photographs reveal late–20th-century dynamic ice loss in northwestern Greenland, *Science*, *337*, 596–573.

Mayer, C., N. Reeh, F. Jung-Rothenhäusler, P. Huybrechts, and H. Orter (2000), The subglacial cavity and implied dynamics under Nioghalvfjerdsfjorden Glacier, NE-Greenland, *Geophys. Res. Lett.*, *27*(15), 2289–2292.

McFadden, E. M., I. M. Howat, I. Joughin, B. Smith, and Y. Ahn (2011), Changes in the dynamics of marine terminating outlet glaciers in west Greenland (2000–2009), *J. Geophys. Res.*, *116*, F02022, doi:10.1029/2010JF001757.

Meier, M. F., and A. Post (1987), Fast tidewater glaciers, *J. Geophys. Res.*, *92*, 9051–9058.

Moon, T., and I. Joughin (2008), Changes in ice-front position on Greenland's outlet glaciers from 1992 to 2007, *J. Geophys. Res.*, *113*, F02022, doi:10.1029/2007JF000927.

Moon, T., I. Joughin, B. E. Smith, and I. M. Howat (2012), 21st-century evolution of Greenland outlet glacier velocities, *Science*, *336*(6081), 576–578.

Motyka, R. J., L. Hunter, K. Echelmeyer, and C. Connor (2003), Submarine melting at the terminus of a temperate tidewater glacier, LeConte Glacier, Alaska, U.S.A., *Ann. Glaciol.*, *36*, 57–65.

Motyka, R. J., M. Truffer, M. Fahnestock, J. Mortensen, S. Rysgaar, and I. M. Howat (2011), Submarine melting of the 1985 Jakobshavn Isbræ floating tongue and the triggering of the current retreat, *J. Geophys. Res.*, *116*, F01007, doi:10.1029/2009JF001632.

Murray, T., et al. (2010), Ocean regulation hypothesis for glacier dynamics in southeast Greenland and implications for ice sheet mass changes, *J. Geophys. Res.*, *115*, F03026, doi:10.1029/2009JF001522.

Nick, F. M., A. Vieli, I. M. Howat, and I. Joughin (2009), Large-scale changes in Greenland outlet glacier dynamics triggered at the terminus, *Nat. Geosci.*, *2*, 110–114.

O'Neel, S., W. T. Pfeffer, R. Krimmel, and M. Meier (2005), Evolving force balance at Columbia Glacier, Alaska, during its rapid retreat, *J. Geophys. Res.*, *110*, F03012, doi:10.1029/2005JF000292.

Partington, K., T. Flynn, D. Lamb, C. Bertoia, and K. Dedrick (2003), Late twentieth century Northern Hemisphere sea-ice record from U.S. National Ice Center ice charts, *J. Geophys. Res.*, *108*(C11), 3343, doi:10.1029/2002JC001623.

Pritchard, H. D., R. J. Arthern, D. G. Vaughan, and L. A. Edwards (2009), Extensive dynamic thinning on the margins of the Greenland and Antarctic ice sheets, *Nature*, *461*, 971–975.

Raymond, C. (1996), Shear margins in glaciers and ice sheets, *J. Glaciol.*, *42*(140), 90–102.

Reynolds, R. W., T. M. Smith, C. Liu, D. B. Chelton, K. S. Casey, and M. G. Schlax (2007), Daily high-resolution-blended analyses for sea surface temperature, *J. Clim.*, *20*(22), 5473–5496, doi:10.1175/2007jcli1824.1.

Rignot, E., and P. Kanagaratnam (2006), Changes in the velocity structure of the Greenland Ice Sheet, *Science*, *311*(5763), 986–990.

Rignot, E., J. E. Box, E. Burgess, and E. Hanna (2008), Mass balance of the Greenland ice sheet from 1958 to 2007, *Geophys. Res. Lett.*, *35*, L20502, doi:10.1029/2008GL035417.

Rignot, E., M. Koppes, and I. Velicogna (2010), Rapid submarine melting of the calving faces of West Greenland glaciers, *Nat. Geosci.*, *3*, 187–191, doi:10.1038/NGEO765.

Rignot, E., I. Velicogna, M. Van den Broeke, A. Monaghan, and J. Lenaerts (2011), Acceleration of the contribution of the Greenland and Antarctic ice sheets to sea level rise, *Geophys. Res. Lett.*, *38*, L05503, doi:10.1029/2011GL046583.

Sasgen, I., M. van den Broeke, J. L. Bamber, E. Rignot, L. S. Sørensen, B. Bert Wouters, Z. Martinech, A. Velicogna, and S. B. Simonseni (2012), Timing and origin of recent regional ice-mass loss in Greenland, *Earth Planet. Sci. Lett.*, *333-334*, 293–303.

Schoof, C. (2007), Ice sheet grounding line dynamics: Steady states, stability, and hysteresis, *J. Geophys. Res.*, *112*, F03S28, doi:10.1029/2006JF000664.

Small, D., B. Rosich, A. Schubert, E. Meier, and D. Nüesch (2004), Geometric validation of low and high-resolution ASAR imagery, *paper presented at 2004 Envisat and ERS Symposium, Salzburg, Austria, 6-10 Sept.*, European Space Agency.

Sohn, H. G., K. C. Jezek, and C. J. van der Veen (1998), Jakobshavn Glacier, West Greenland: 30 years of spacebourne observations, *Geophys. Res. Lett.*, *25*(14), 2699–2702.

Straneo, F., G. S. Hamilton, D. A. Sutherland, L. A. Stearns, F. Davidson, M. O. Hammill, G. B. Stenson, and A. R. Asvid (2010), Rapid circulation of warm subtropical waters in a major glacial fjord in East Greenland, *Nat. Geosci.*, *3*, 182–186, doi:10.1038/NGEO764.

Straneo, F., R. G. Curry, D. A. Sutherland, G. S. Hamltion, C. Cenedese, K. Våge, and L. A. Stearns (2011), Impact of fjord dynamics and glacial runoff on the circulation near Helheim Glacier, *Nat. Geosci.*, *4*, 322–327.

Thomas, R. H., E. Frederick, W. Krabill, S. Manizade, and C. Martin (2009), Recent changes on Greenland outlet glaciers, *J. Glaciol.*, *55*(189), 147–162.

van den Broeke, M., J. Bamber, J. Ettema, E. Rignot, E. Schrama, W. J. van de Berg, E. van Meijgaard, I. Velicogna, and B. Wouters (2009), Partitioning recent Greenland mass loss, *Science*, *326*, 984–986.

van der Veen, C. J. (1998), Fracture mechanics approach to penetration of bottom crevasses on glaciers, *Cold Reg. Sci. Technol.*, *27*, 213–223.

Veitch, S. A., and N. Nettles (2012), Spatial and temporal variations in Greenland glacial-earthquake activity, 1993–2010, *J. Geophys. Res.*, *117*, F04007, doi:10.1029/2012JF002412.

Vieli, A., and F. M. Nick (2011), Understanding and modelling rapid dynamic changes of tidewater outlet glaciers: Issues and implications, *Surv. Geophys.*, *32*, 437–485.

Vieli, A., M. Funk, and H. Blatter (2001), Flow dynamics of tidewater glaciers: A numerical modelling approach, *J. Glaciol.*, *47*(159), 595–606.

Vieli, A., J. A. Jania, and K. Lezek (2002), The retreat of a tidewater glacier: Observations and model calculations on Hansbreen, Spitsbergen, *J. Glaciol.*, *48*(163), 592–600.

Warren, C. R., and N. F. Glasser (1992), Contrasting response of south Greenland glaciers to recent climatic change, *Arct. Alp. Res.*, *24*(2), 124–132.

Weertman, J. (1974), Stability of the junction of an ice sheet and an ice shelf, *J. Glaciol.*, *13*(67), 3–11.